Facile synthesis of zeolitic imidazolate framework coated glass microspheres

Ashleigh M. Chester[a†], Celia Castillo-Blas[a‡], Luke Woodliffe[b], Md Towhidul Islam[b], Jesús Molinar-Díaz[b], Andi Arjuna[b,c], Emma Barney[b], Ifty Ahmed[b], Andrea Laybourn[b,d*], David A. Keen[e] and Thomas D. Bennett[a,f*].

[a]*Department of Materials Science and Metallurgy, University of Cambridge, Cambridge, CB3 0FS, UK.*

[b]*Advanced Materials Research Group, Faculty of Engineering, University of Nottingham, Nottingham NG7 2RD, UK.*

[c]*Department of Pharmaceutical Sciences and Technology, Faculty of Pharmacy, Hasanuddin University, Makassar, 90245.*

[d]*Institute of Process Research and Development & School of Chemistry, University of Leeds, Leeds, LS2 9JT, UK.*

[e]*ISIS Facility, Rutherford Appleton Laboratory, Harwell Campus, Didcot, Oxfordshire OX11 0QX, UK.*

[f]*MacDiarmid Institute for Advanced Materials and Nanotechnology, School of Physical and Chemical Sciences, University of Canterbury, Private Bag 4800, Christchurch 8140, New Zealand.*

*Corresponding author email: thomas.bennett@canterbury.ac.nz; A.Laybourn@leeds.ac.uk

Table of Contents

1. Characterisation of P40 glass microspheres

Solid microspheres (SMS) and porous microsphere (PMS) batches were characterised by PXRD, FTIR, SEM-EDX, TGA and DSC.

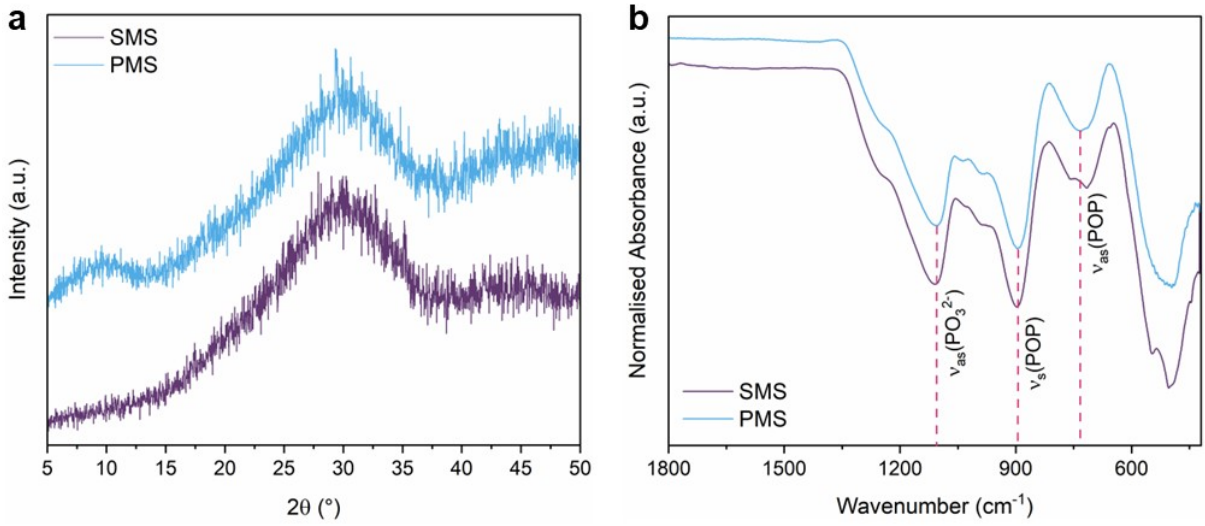

Figure S1. a. PXRD patterns and **b.** FTIR spectra of solid (SMS) and porous microspheres (PMS).

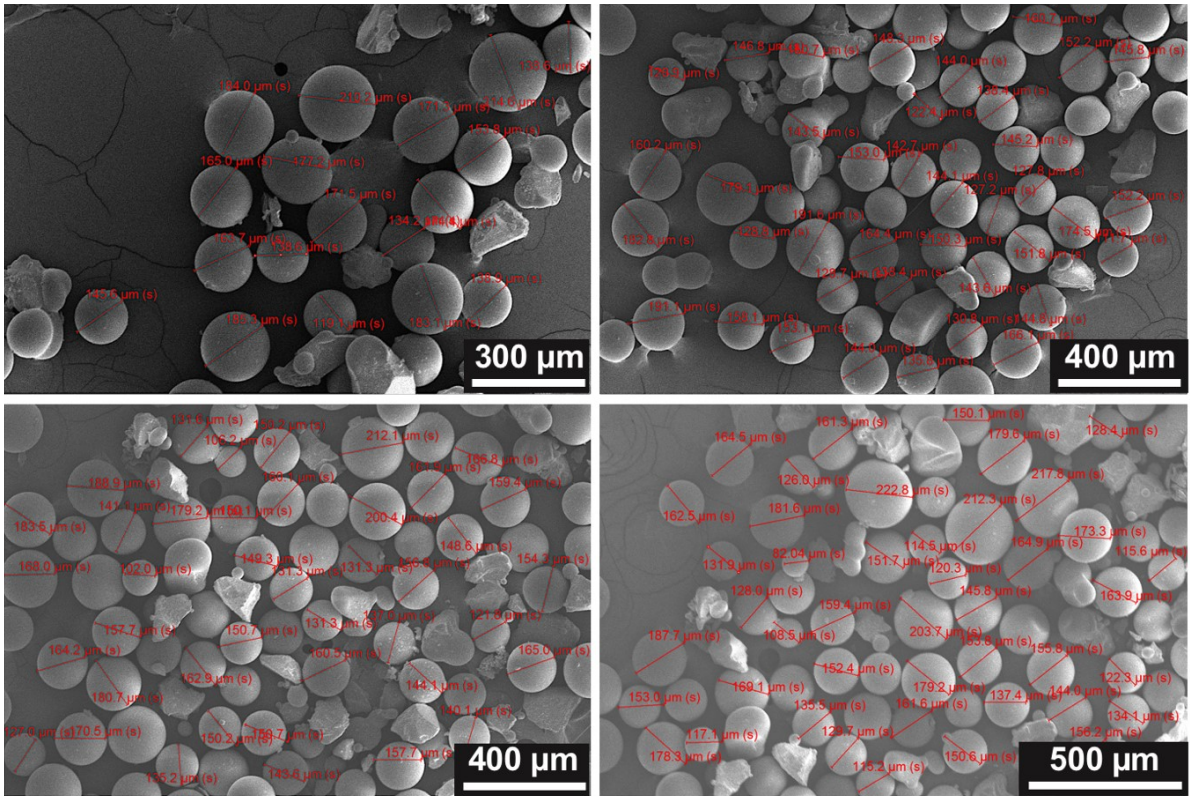

Figure S2. SEM images used to calculate the size distribution of the SMS (142 microspheres). The four panels shown indicate four different regions of the SMS sample used to analyse the size distribution. See Figure S4 for histogram plot showing microsphere sizes.

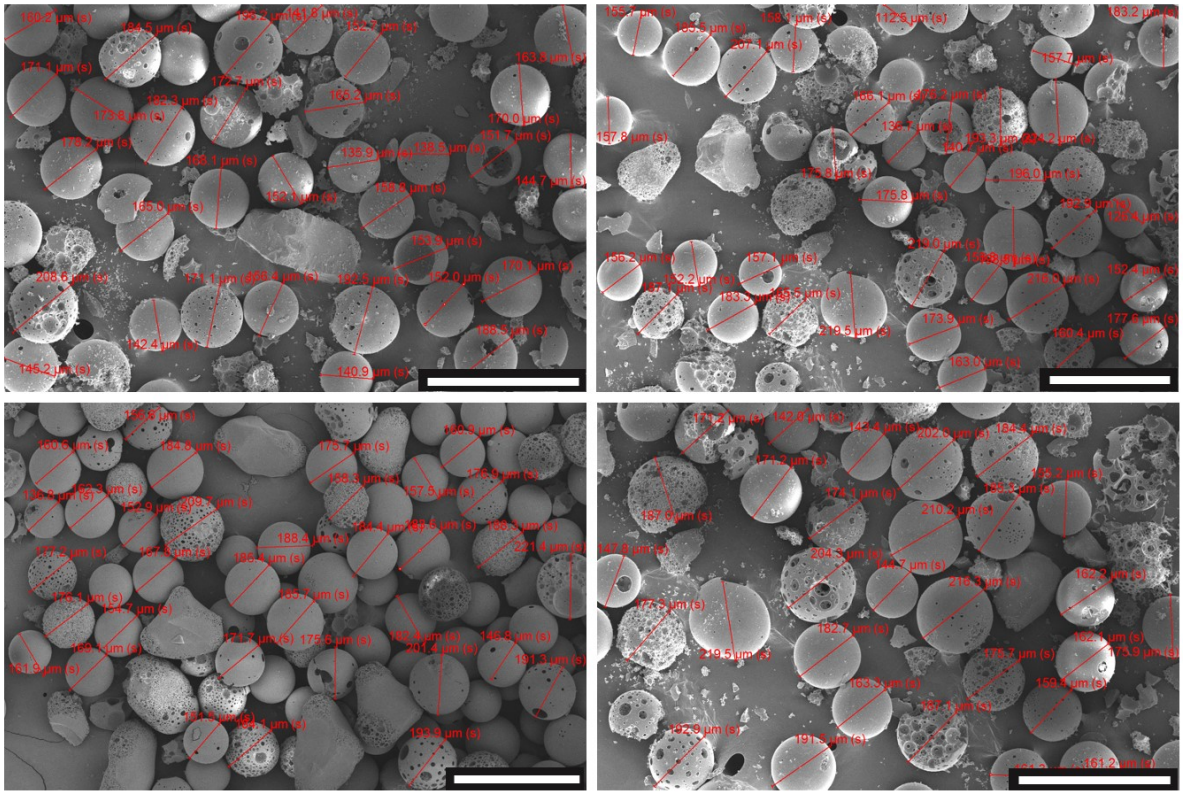

Figure S3. SEM images used to calculate the size distribution of PMS (129 microspheres, scale bar: 400 μm). The four panels shown indicate four different regions of the PMS sample used to analyse the size distribution. The sample was coated in silver. See Figure S4 for histogram plot showing microsphere sizes.

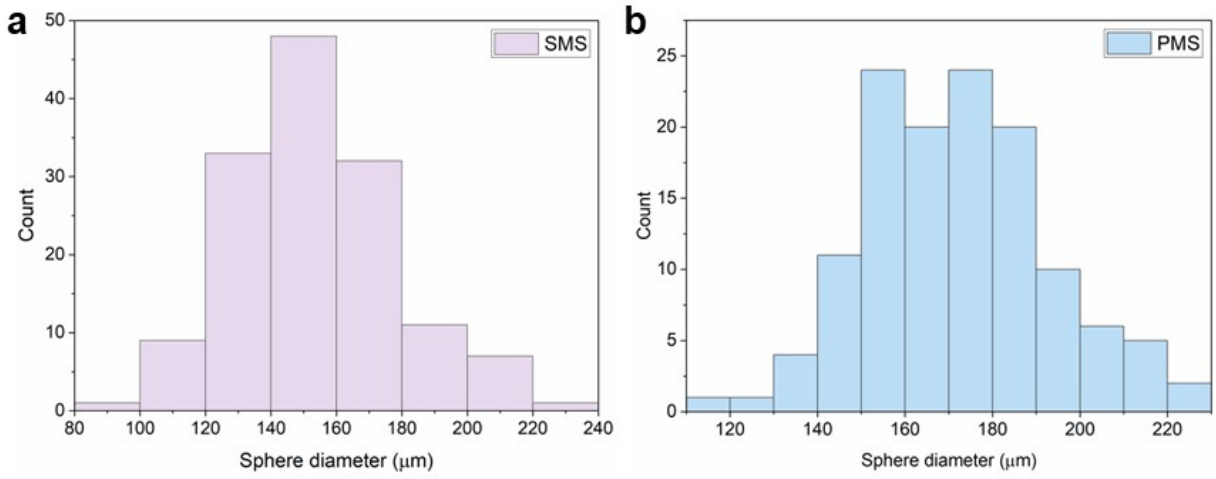

Figure S4. Average diameters of **a.** SMS, with a mean particle diameter of 152.9 ± 24.8 μm and **b.** PMS, with a mean particle diameter of 171.5 ± 21.4 μm.

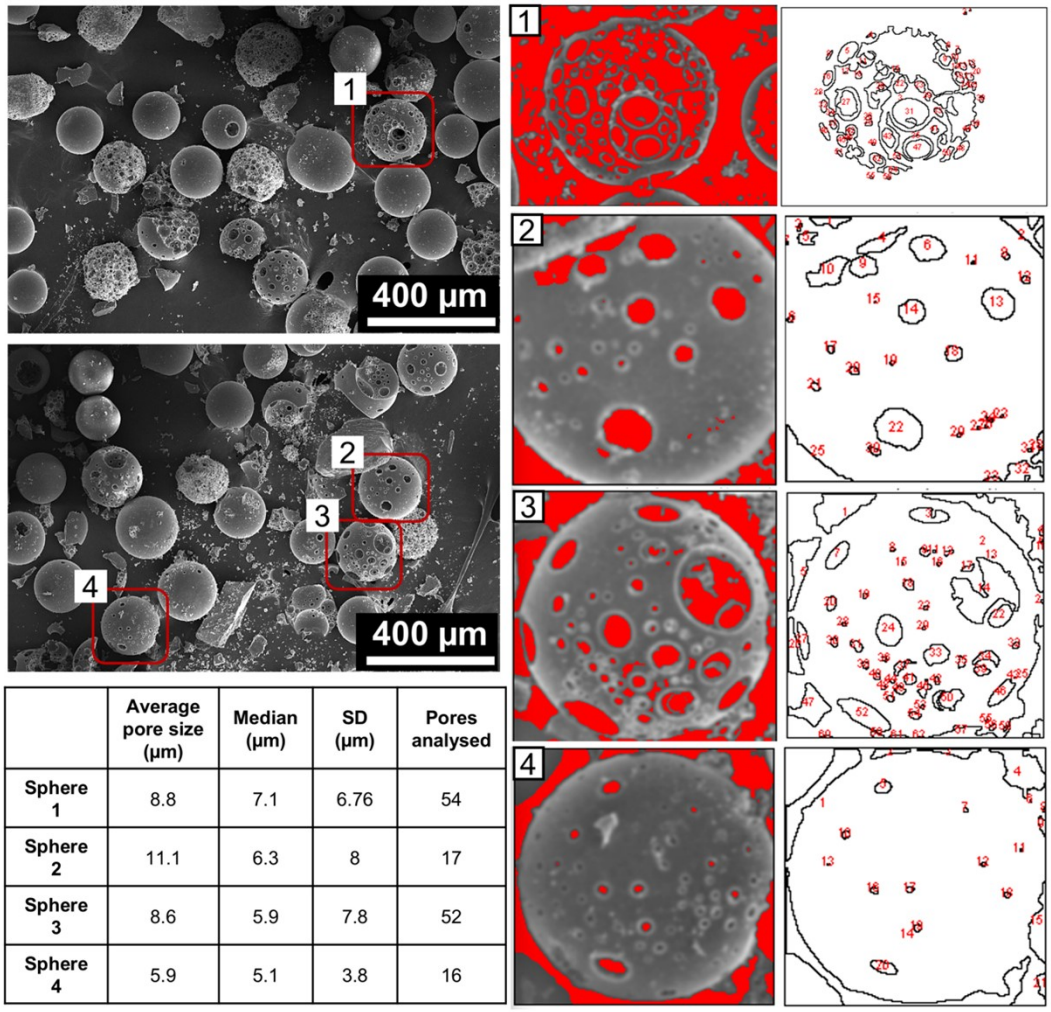

	Average pore size (µm)	Median (µm)	SD (µm)	Pores analysed
Sphere 1	8.8	7.1	6.76	54
Sphere 2	11.1	6.3	8	17
Sphere 3	8.6	5.9	7.8	52
Sphere 4	5.9	5.1	3.8	16

Figure S5. SEM images used in ImageJ to determine the pore diameter distribution of PMS (total of 139 pores sampled from 4 separate microspheres), SD = Standard deviation.

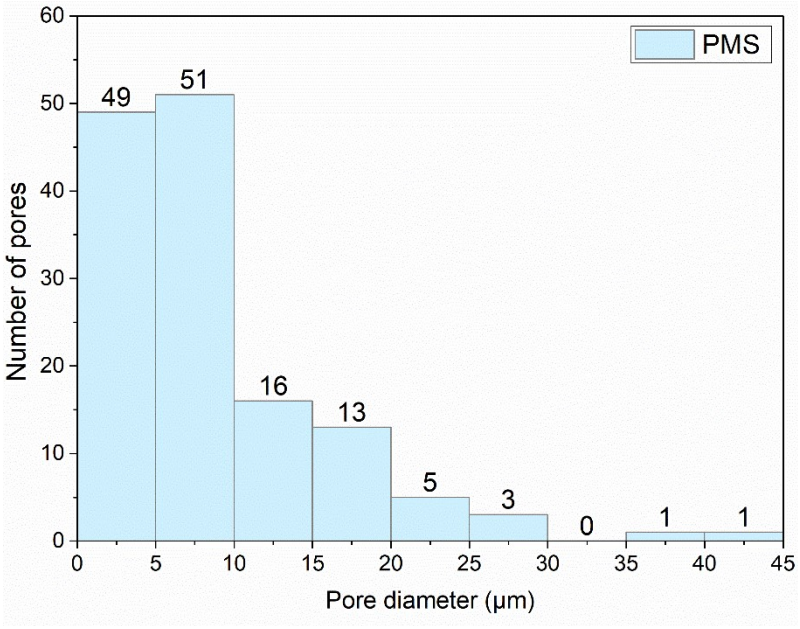

Figure S6. Pore diameter distribution of PMS, average pore diameter: 8.7 ± 7.1 µm (median: 6.3 µm, minimum 1.2 µm, maximum 43.4 µm).

SEM-EDS was used to determine the compositions of the glasses (**Table S1**). The % of O and Ca could not be accurately determined; high deviations from the nominal O and Ca composition were observed.

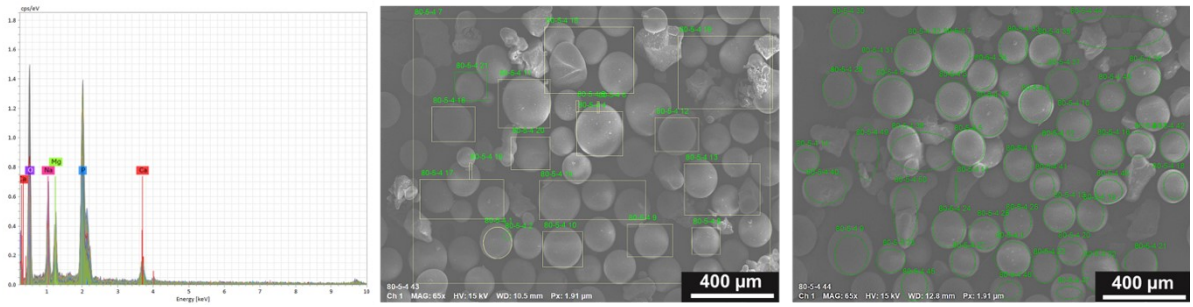

Figure S7. Areas used to calculate the composition of the solid microspheres by SEM-EDS.

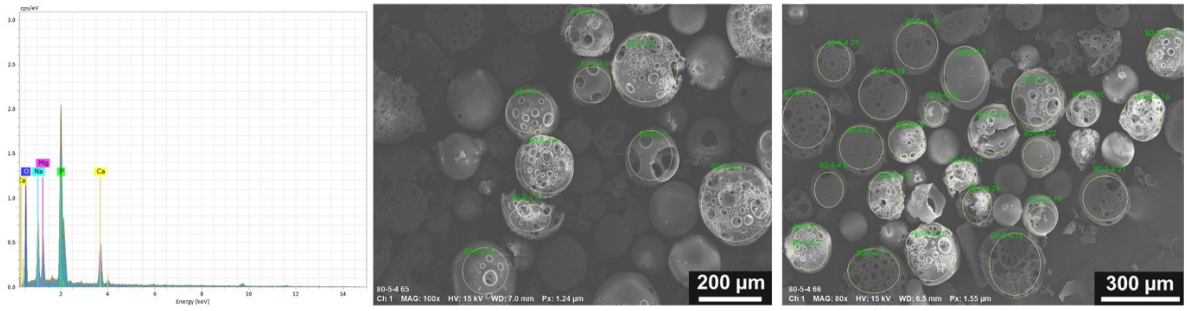

Figure S8. Areas used to calculate the composition of the PMS by SEM-EDS.

Table S1. Elemental composition of SMS and PMS determined by SEM-EDS.

	% Mg	% Na	% P
Nominal	**5.714**	**9.524**	**19.048**
SMS	5.7 ± 0.6	8.9 ± 1.0	20.9 ± 1.4
PMS	5.4 ± 0.8	7.9 ± 1.0	21.9 ± 2.6

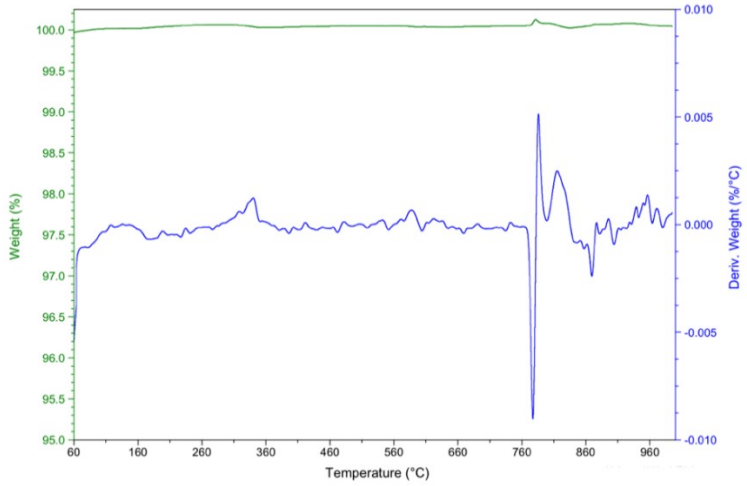

Figure S9. TGA thermogram of the pristine SMS measured by heating the sample to 1000 ºC.

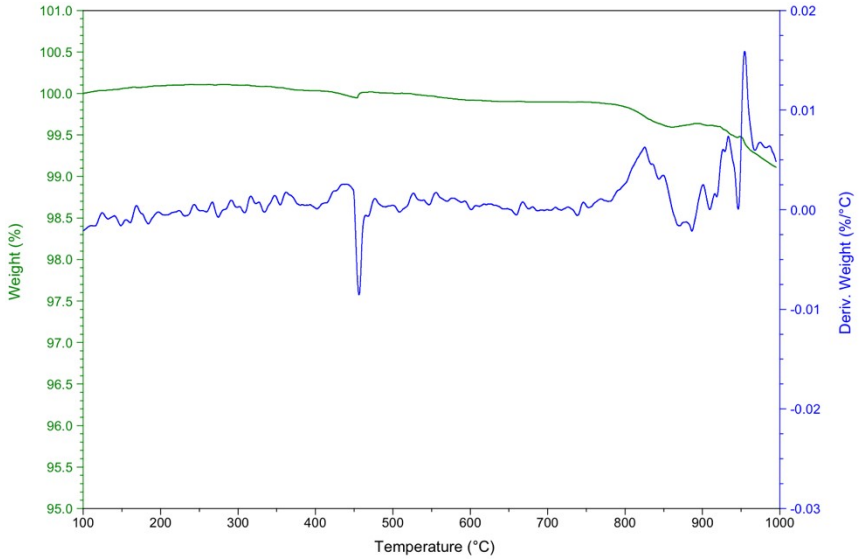

Figure S10. TGA thermogram of PMS measured by heating the sample to 1000 ºC.

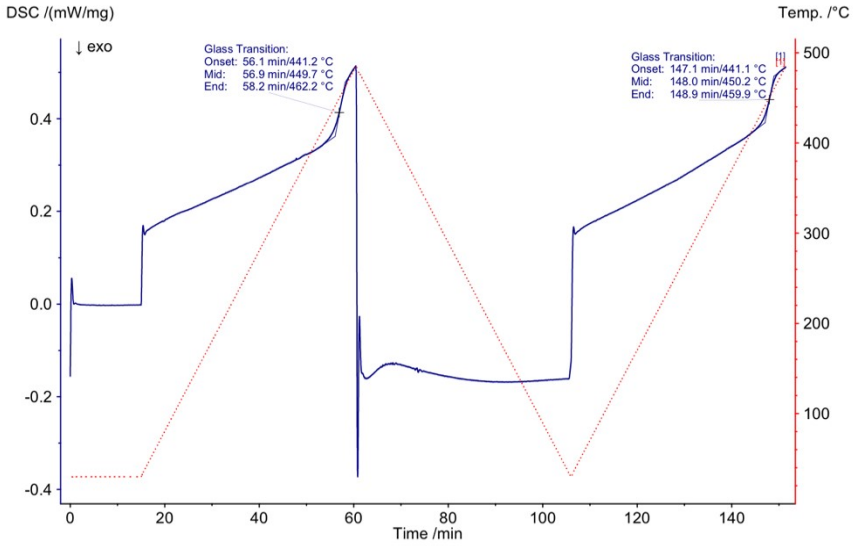

Figure S11. Full DSC scan of the pristine SMS.

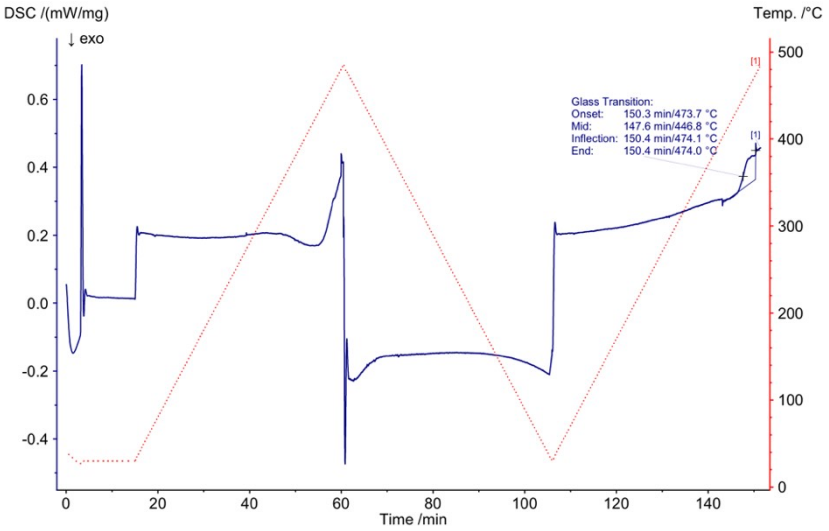

Figure S12. Full DSC scan of the pristine PMS.

2. SEM images of ZIF-8@solid microspheres composites

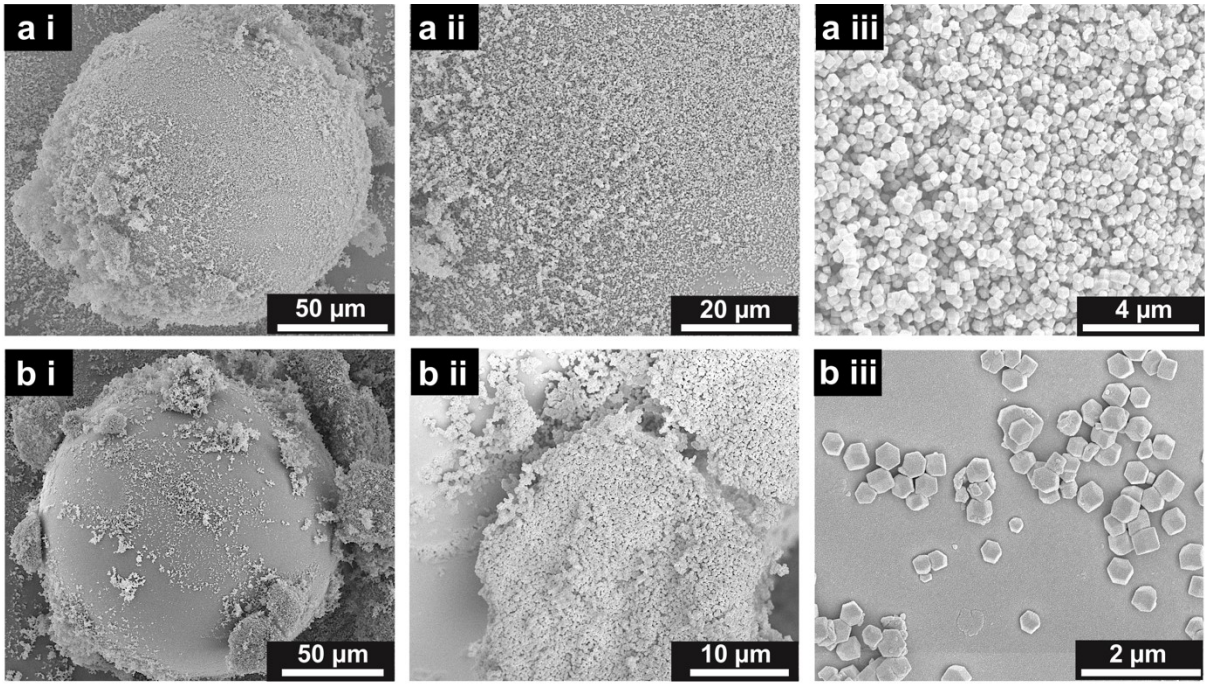

Figure S13. SEM images of the ZIF-8@SMS_4.5hr composite. Figures **a** and **b** show two different spheres with ZIF-8 coating the surfaces. Images **a ii**, **a iii**, **b ii** and **b iii** correspond to the same spheres in **a** and **b** but at higher magnification.

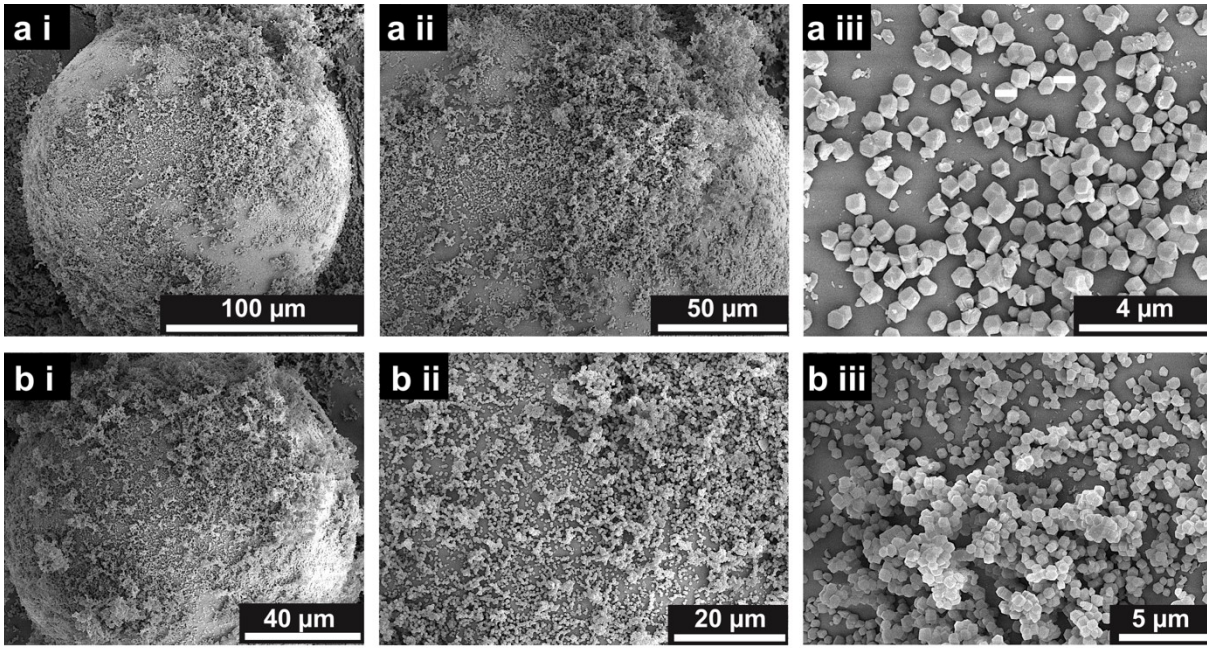

Figure S14. SEM images of the ZIF-8@SMS_2hr composite. Figures **a** and **b** show two different spheres with ZIF-8 coating the surfaces. Images **a ii**, **a iii**, **b ii** and **b iii** correspond to the same spheres in **a** and **b** but at higher magnification.

3. SEM images of ZIF-8@porous microspheres composites

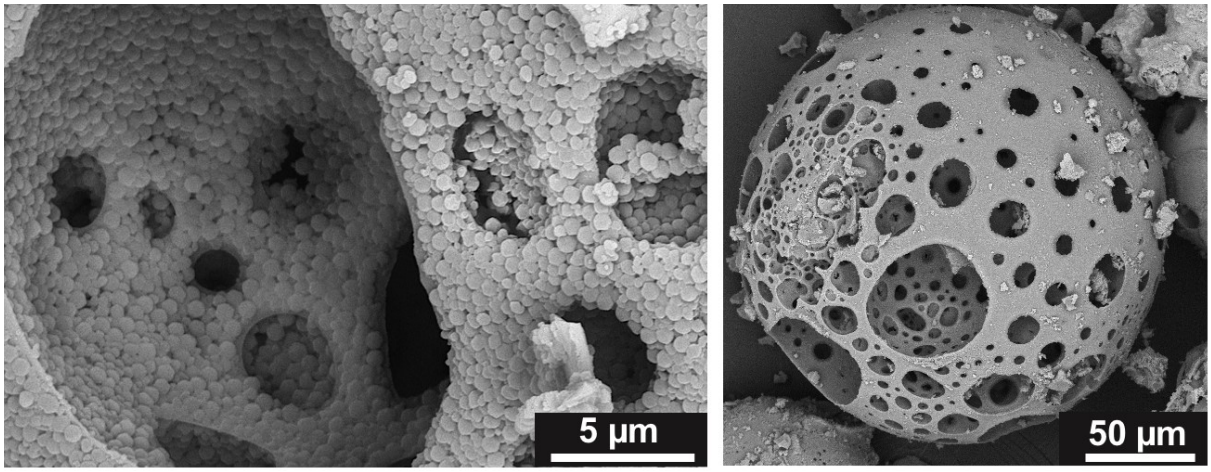

Figure S15. SEM images of the ZIF-8@PMS_1hr composite. Images correspond to the same sphere but at different magnifications.

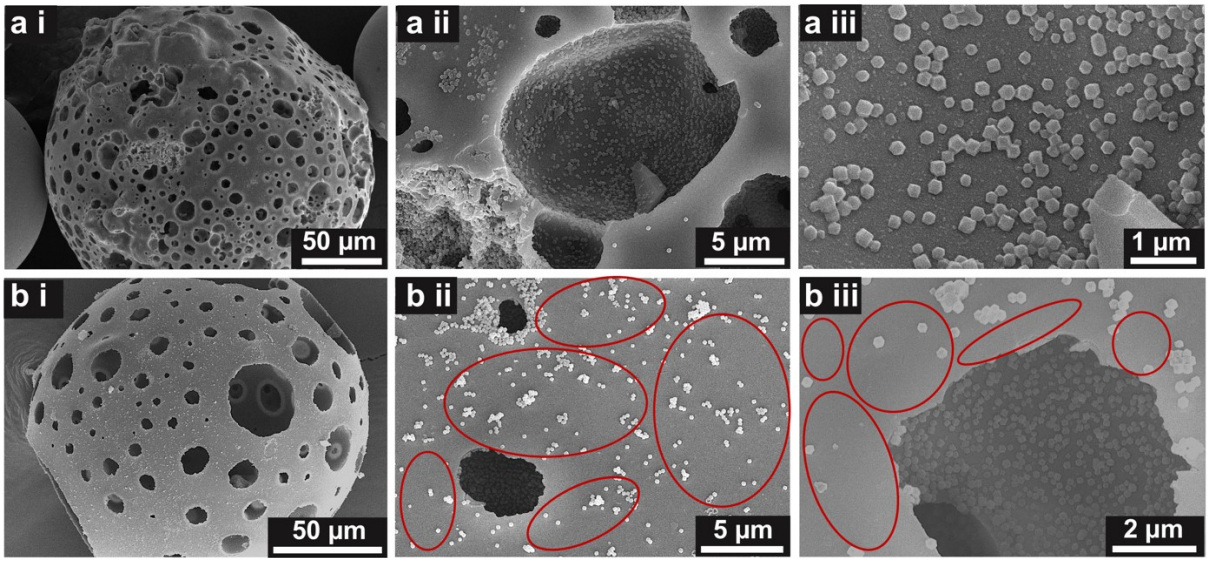

Figure S16. SEM images of the ZIF-8@PMS_1hr composite. Two different spheres are shown in images **a i** and **b i**. Images **a ii-iii** and **b ii-iii** show the same sphere but at higher magnification; red circles indicate example regions on the microspheres' surfaces where the ZIF-8 coating is less homogenous.

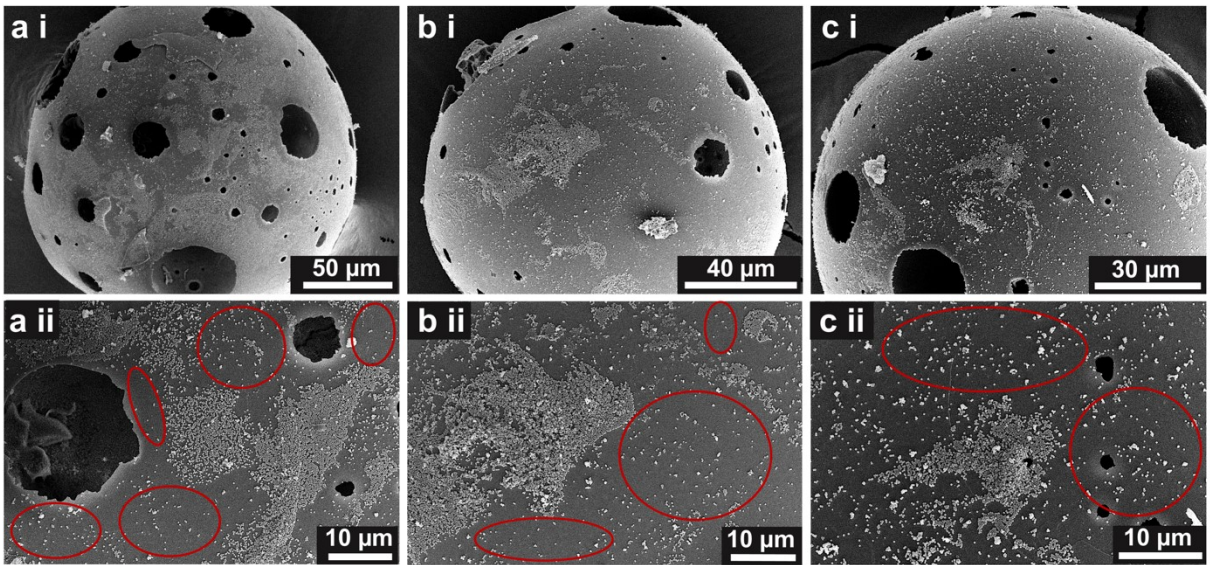

Figure S17. SEM images of the ZIF-8@PMS_2hr composite. Three different spheres are shown in images **a i**, **b i** and **c i**. Images **a ii**, **b ii** and **c ii** show the same spheres in **a i**, **b i** and **c i** but at higher magnification; red circles indicate example regions on the microspheres' surfaces where the ZIF-8 coating is less homogenous.

4. Characterisation and properties of ZIF-8@microphere composites

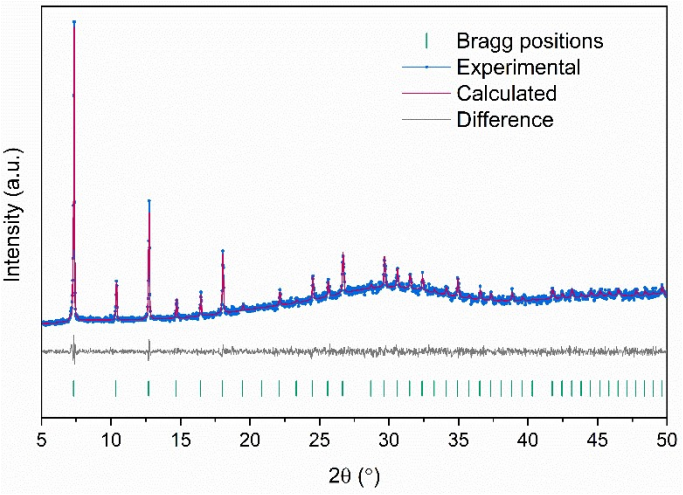

Figure S18. Pawley refinement of the PXRD diffraction data of the ZIF-8@SMS_1hr composite. Experimental (pink dots), calculated (blue line), difference plot [(I_{obs}−I_{calc})] (grey line) and Bragg positions (green ticks) obtained from the Pawley refinement of experimental diffraction data of pristine ZIF-8 (space group: *I-43m*) for 2θ = 5-50°. Literature lattice parameter, *a* = 16.8509(3).[2]

Table S2. Pawley refinement details of ZIF-8@SMS_1hr composite.

R_{wp}	Space group	Zero error (°)	Profile parameters	Lattice parameter, *a* (Å)
7.35%	*I-43m*	0.037(16)	U: 0.61(37) V: -0.21(12) W: 0.011(7)	17.015(4)

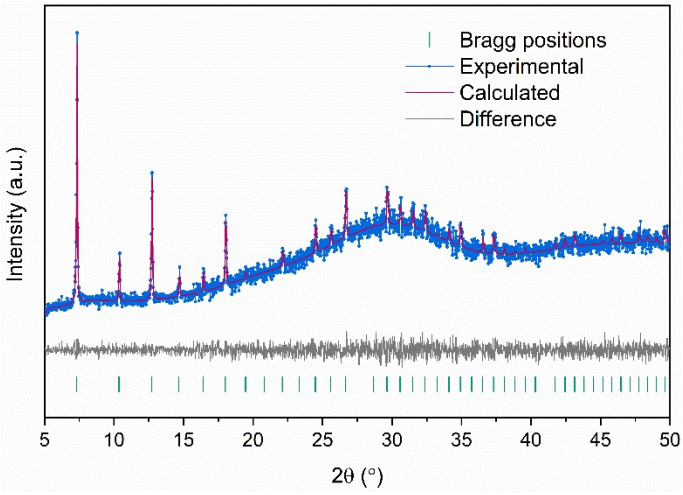

Figure S19. Pawley refinement of the PXRD data of the ZIF-8@PMS_4.5hr composite. Experimental (pink dots), calculated (blue line), difference plot [(I_{obs}−I_{calc})] (grey line) and Bragg positions (green ticks) obtained from the Pawley refinement of experimental diffraction data of pristine ZIF-8 (space group: *I-43m*) for 2θ = 5-50°. Literature lattice parameter, *a* = 16.8509(3).[2]

Table S3. Pawley refinement details of ZIF-8@PMS_4.5hr composite.

R_{wp}	Space group	Zero error (°)	Profile parameters	Lattice parameter, *a* (Å)
8.1%	*I-43m*	0.05(27)	U: 0.54(45) V: -0.22(17) W: 0.012(100)	17.027(7)

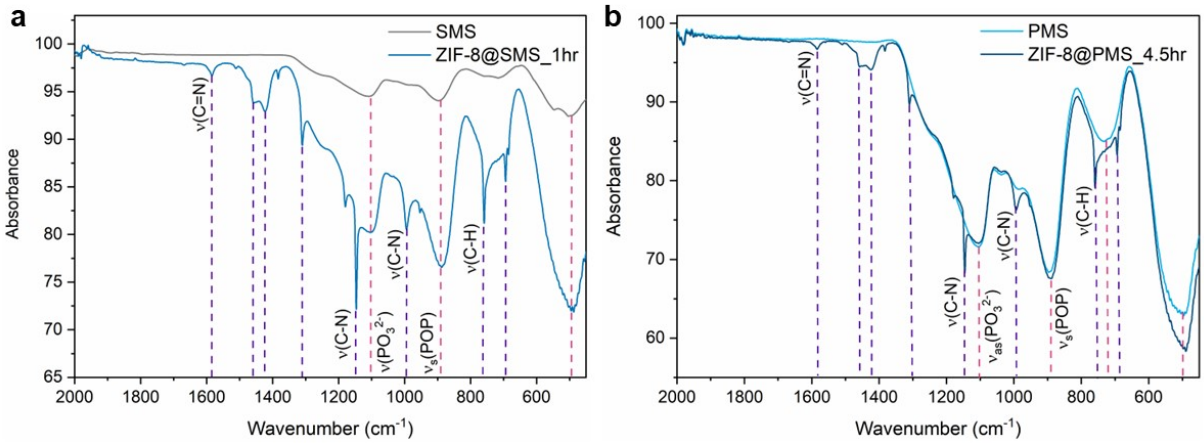

Figure S20. ATR-FTIR spectra of **a.** ZIF-8@SMS_1hr composite and SMS and **b.** ZIF-8@PMS_4.5hr composite and pristine PMS. Purple and pink dashed lines indicate bands from ZIF-8 and pristine microspheres respectively.

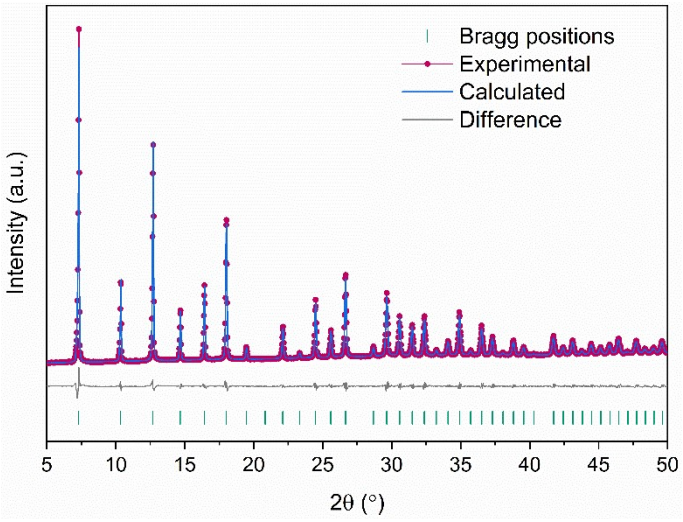

Figure S21. Pawley refinement of the PXRD data of the pristine ZIF-8 control. Experimental (pink dots), calculated (blue line), difference plot [(I_{obs}−I_{calc})] (grey line) and Bragg positions (green ticks) obtained from the Pawley refinement of experimental diffraction data of pristine ZIF-8 (space group: *I-43m*) for 2θ = 5-50°. Literature lattice parameter, *a* = 16.8509(3).[2]

Table S4. Pawley refinement details of the pristine ZIF-8 control.

R_{wp}	Space group	Zero error (°)	Profile parameters	Lattice parameter, *a* (Å)
6.2%	*I-43m*	0.007(30)	U: -0.03(2) V: 0.36(6) W: -0.003(50)	17.0327(3)

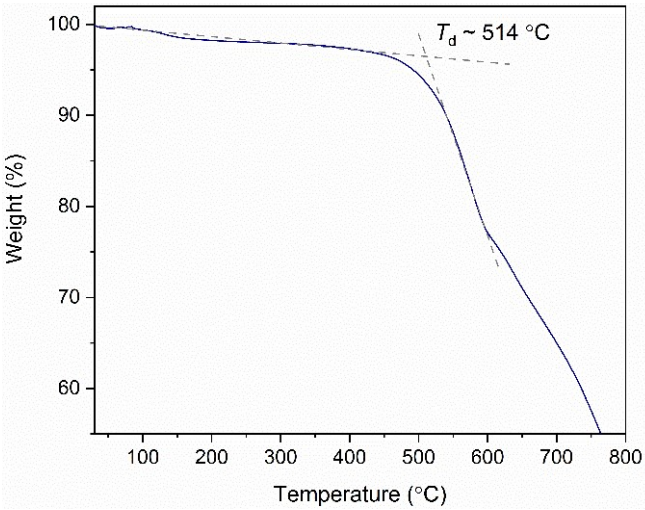

Figure S22. TGA thermogram of the pristine ZIF-8 control measured by heating the sample to 800 ºC.

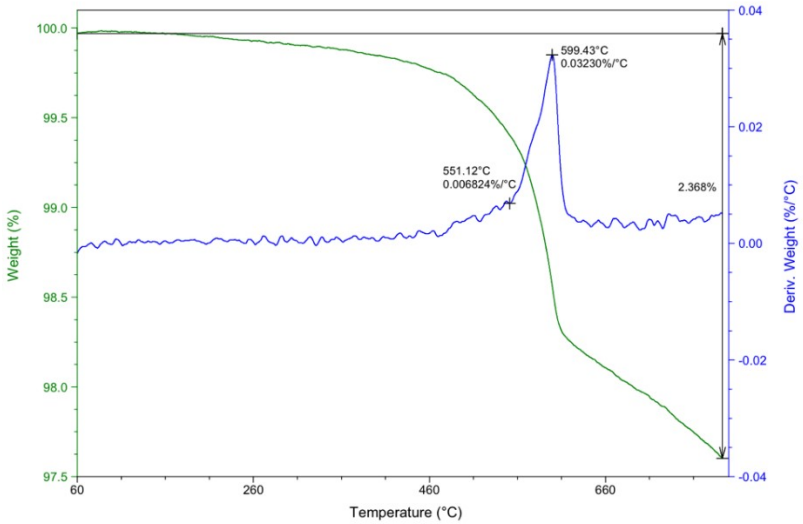

Figure S23. TGA thermogram of the ZIF-8@SMS_1hr composite measured by heating the sample to 800 ºC.

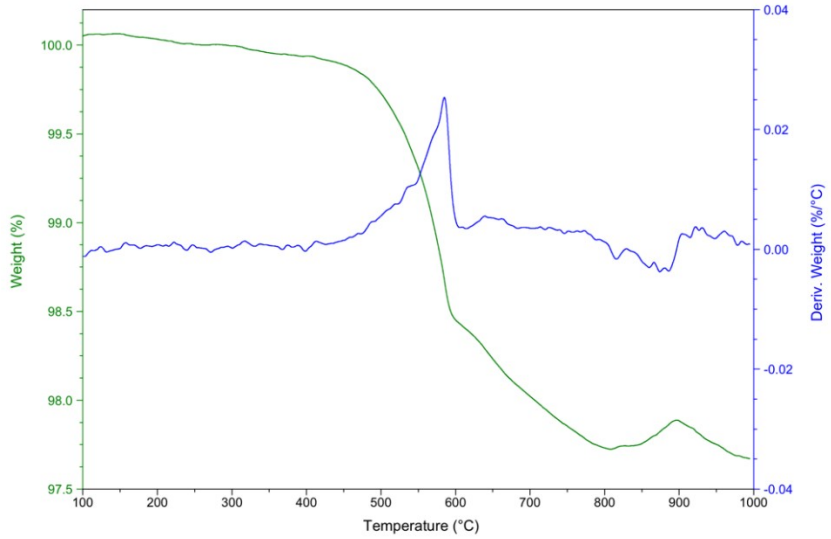

Figure S24. TGA thermogram of the ZIF-8@PMS_4.5hr composite measured by heating the sample to 1000 ºC.

The amount of ZIF-8 on the surface of the microspheres can be estimated by considering the temperature at which pristine ZIF-8 decomposed, 790.5 ºC (**Figure S22**):

$$\text{Estimated ZIF-8 mass \%} = \frac{\text{\% Mass loss of composite at T = 790.5 ºC}}{\text{Mass loss of pristine ZIF - 8 at T = 790.5 ºC}}$$

For the ZIF-8@SMS_1hr composite, estimated ZIF-8 mass is $\frac{2.239}{0.4962}$ ~ 4.51%. This assumes negligible decomposition of the solid microspheres (weight% is 100 at T = 790.5 ºC).

For the ZIF-8@PMS_4.5hr composite, estimated ZIF-8 mass is $\frac{2.253}{0.4962}$ ~ 4.54% (weight% for pristine porous microspheres at T = 790.5 ºC is 99.86).

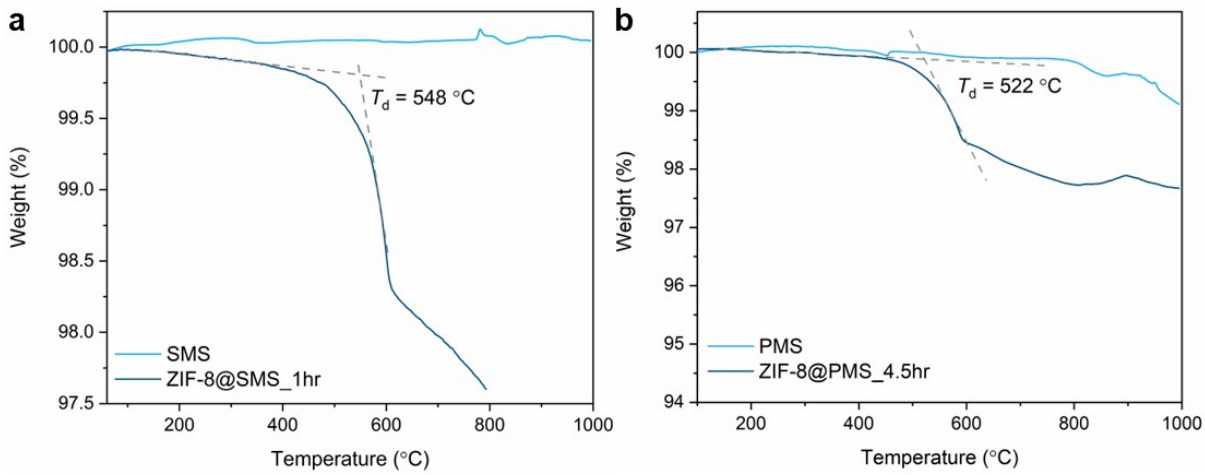

Figure S25. TGA thermogram of **a.** SMS and ZIF-8@ SMS_1hr composite and **b.** ZIF-8@PMS_4.5hr composite and PMS.

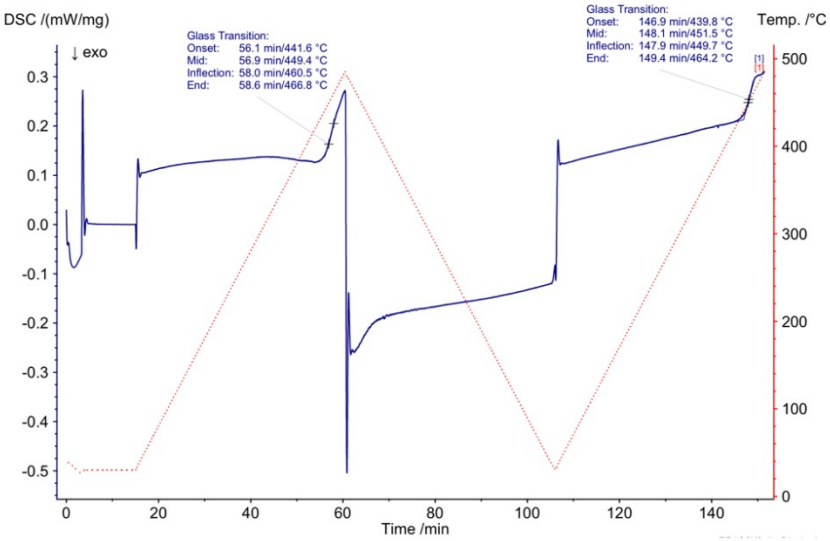

Figure S26. Full DSC scan of the ZIF-8@SMS_1hr composite.

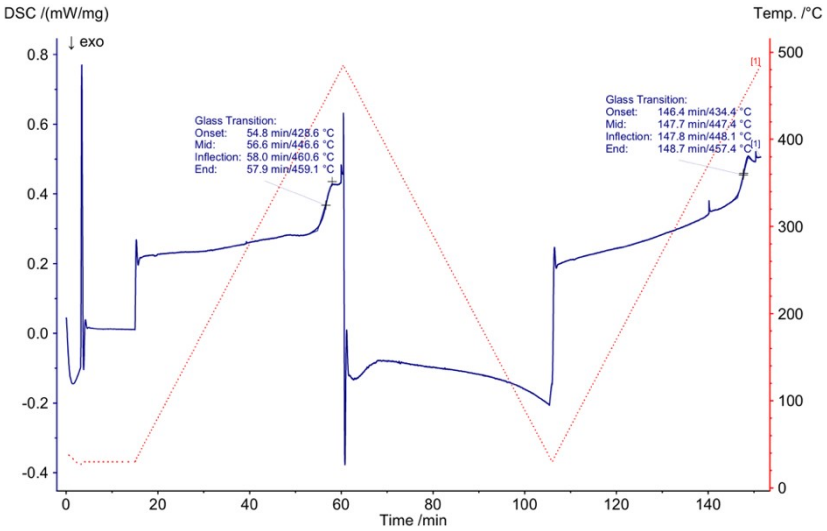

Figure S27. Full DSC scan of the ZIF-8@PMS_4.5hr composite.

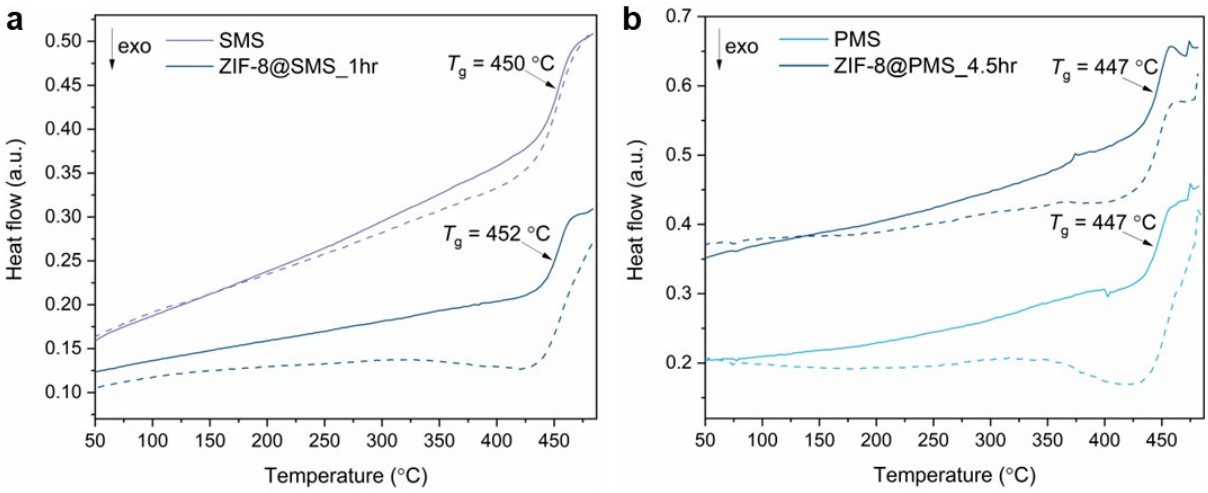

Figure S28. DSC upscans of **a.** ZIF-8@SMS_1hr composite and SMS and **b.** ZIF-8@PMS_4.5hr composite and PMS. Dashed and solid lines represent the first and second DSC upscans respectively.

5. Assessing suitability for biomedical applications

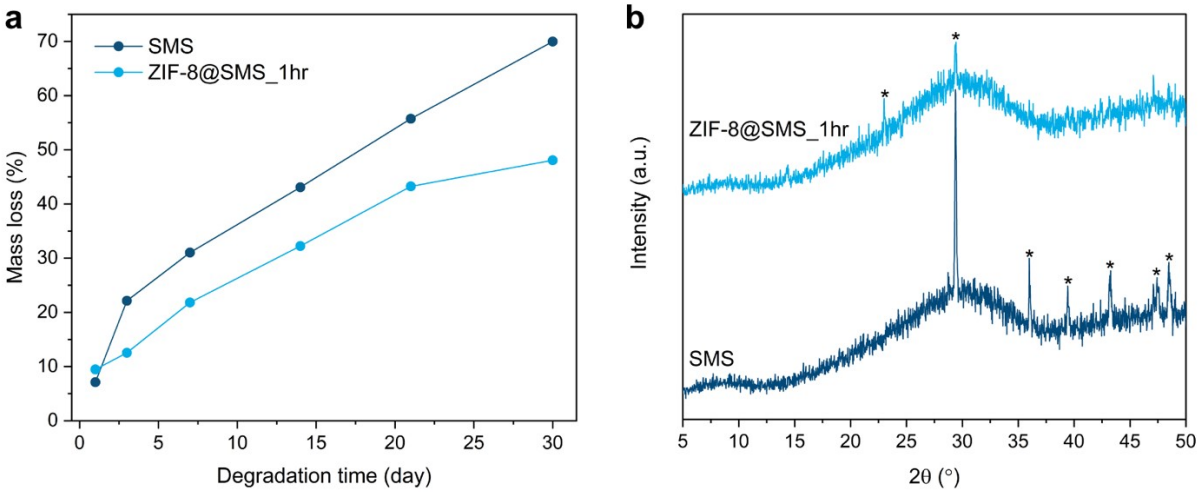

Figure S29. a. Mass loss of the solid microspheres and the ZIF-8@SMS_1hr composite immersed in ultrapure water over a 30-day period and **b.** PXRD of samples post immersion in ultrapure water after 30 days, showing $CaCO_3$ peaks (*) (calcite, CCDC 1865151),[1] likely formed from the reaction of Ca^{2+} ions released from the glass and HCO_3^- from the dissolution of atmospheric CO_2.[3] A small peak is visible at 2θ ~15 °; although this is close to the position of the (220) Bragg peak from ZIF-8 such an assignment is unlikely as the strongest ZIF-8 Bragg peak is the 110 peak at 2θ ~7.5 ° which is not present here. Masses recorded can be found in Table S5.

Table S5. Masses of recovered solid microspheres and the ZIF-8@SMS_1hr composite after immersion in ultrapure water over a 30 day period.

Day	Mass (mg) SMS	Mass (mg) ZIF-8@SMS_1hr
0	50.6	51.8
1	47	46.9
3	39.4	45.3
7	34.9	40.5

14	28.8	35.1
21	22.4	29.4
30	15.2	26.9

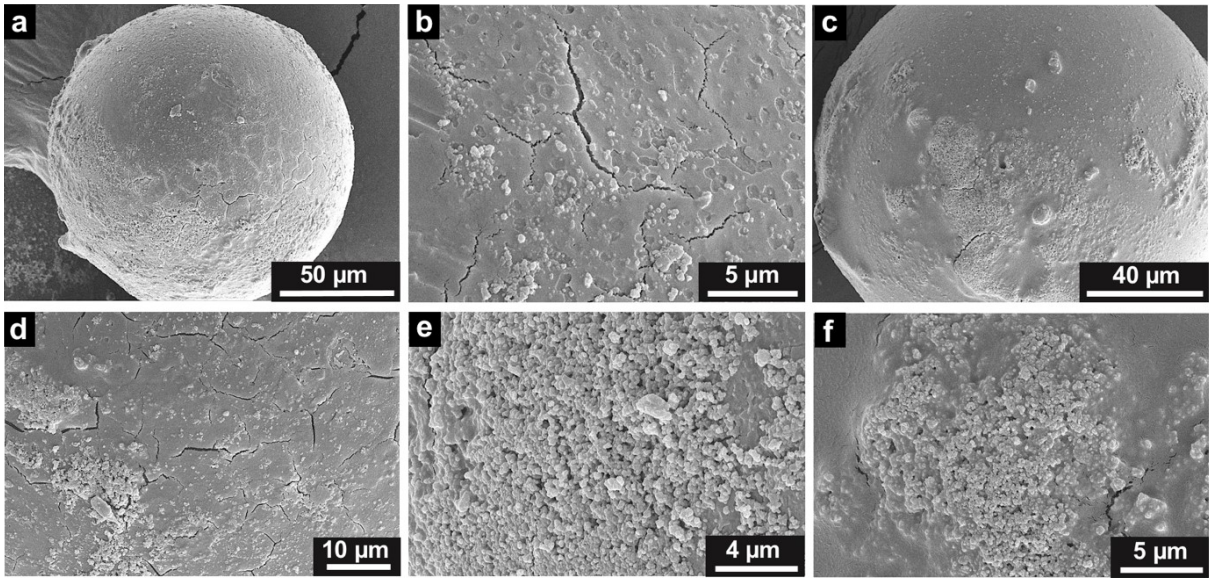

Figure S30. SEM images of three separate spheres of the ZIF-8@SMS_1hr composite after 30 days in ultra-pure water (**a, b, c**). Images in **d** and **f** are images of spheres in **a** and **c** (directly above) while images **b** and **e** are images of different sections of the same sphere, different to the spheres in **a** and **c**.

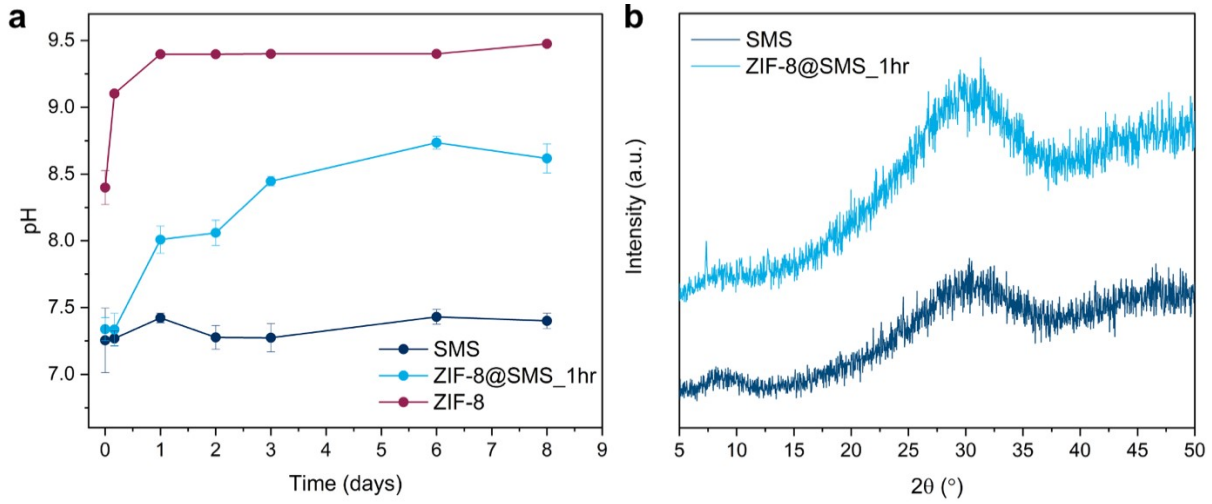

Figure S31. a. Changes in pH of the PBS solutions containing solid microspheres (SMS) and the ZIF-8@SMS_1hr composite over eight days and **b.** PXRD patterns of samples recovered after eight days immersion in PBS, Bragg peak at 2θ ~7.5 ° likely corresponds to the 110 reflection of ZIF-8. T= 0 (Day 0) refers to the pH at the start of the experiments. The second time point is at 4 hours immersion, when the pH had stabilised. Error bars (standard deviation) are shown; where they are not visible, it is because they are too small to be distinguished from the data points.

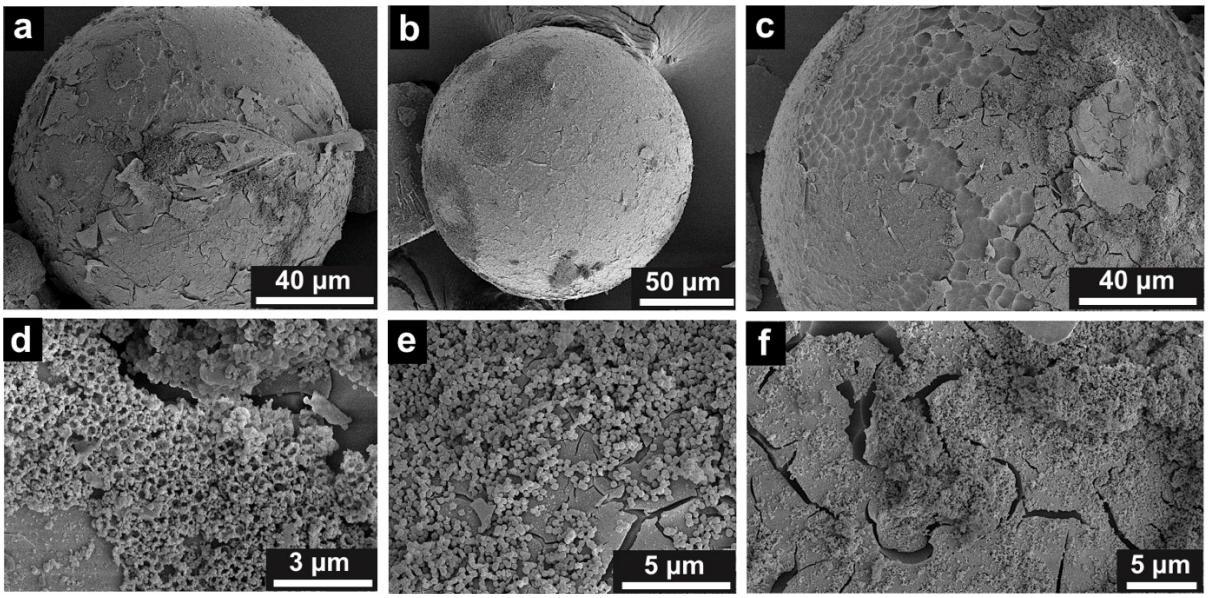

Figure S32. SEM images of three spheres of the ZIF-8@SMS_1hr composite after eight days immersion in PBS (**a**, **b**, **c**). Images in **d**, **e**, **f** show the same spheres as the images directly above but at higher magnification. The degradation and morphological changes were not consistent across the microspheres in and some spheres in the ZIF-8@SMS_1hr composite show the continued presence of ZIF-8 on the surface, with no discernible shape changes.

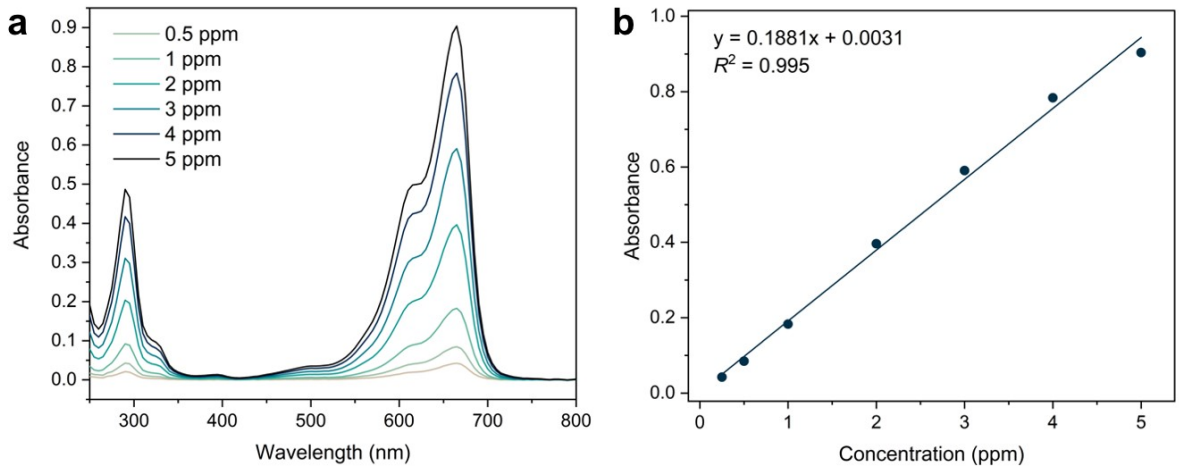

Figure S33. a. UV-VIS spectra of variable MB concentrations used for calibration and **b.** Obtained calibration curve using MB absorbance at 665 nm (error bars are smaller than the data points).

Table S6. Absorbances of aqueous MB solutions after contact with SMS and ZIF-8@SMS_1hr composite samples, remaining dye concentration (ppm) and calculated dye adsorbed from the stock solution (5 ppm).

Sample	Absorbance at 665 nm	Dye remaining (ppm)	Dye adsorbed (%)
SMS	0.838(3)	4.437	11.3
ZIF-8@SMS_1hr	0.789(3)	4.176	16.5

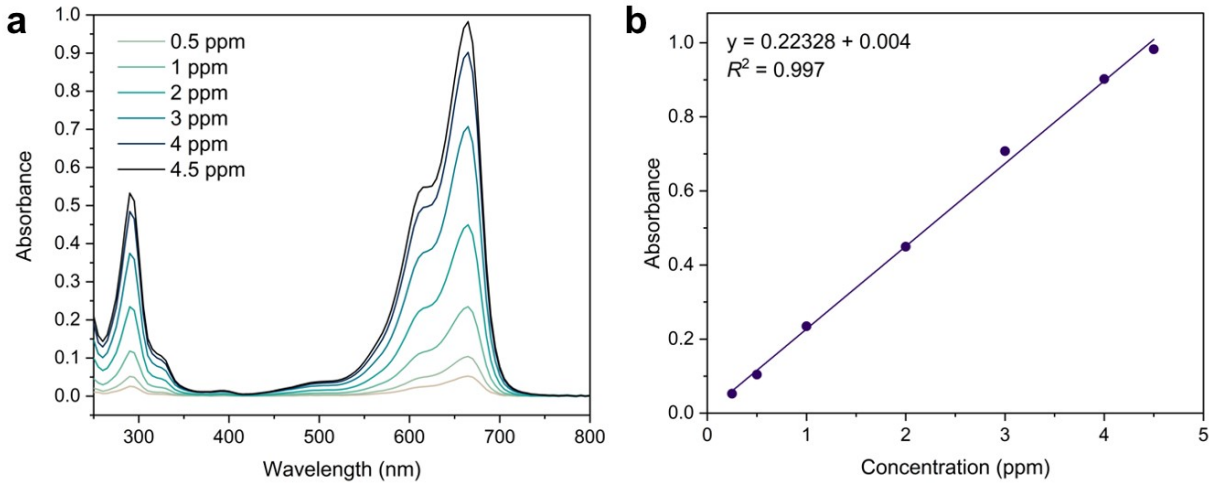

Figure S34. a. UV-VIS spectra of variable MB concentrations used for calibration and **b.** Obtained calibration curve using MB absorbance at 665 nm (error bars are smaller than the data points) for the PMS and ZIF-8@PMS_4.5hr composite experiments.

Table S7. Absorbances of aqueous MB solutions after contact with PMS and ZIF-8@PMS_4.5hr samples, remaining dye concentration (ppm) and calculated dye adsorbed from the stock solution (5 ppm).

Sample	Absorbance at 665 nm	Dye remaining (ppm)	Dye adsorbed (%)
PMS	0.912(5)	4.07	18.7
ZIF-8@PMS_4.5hr	0.846(2)	3.77	24.6

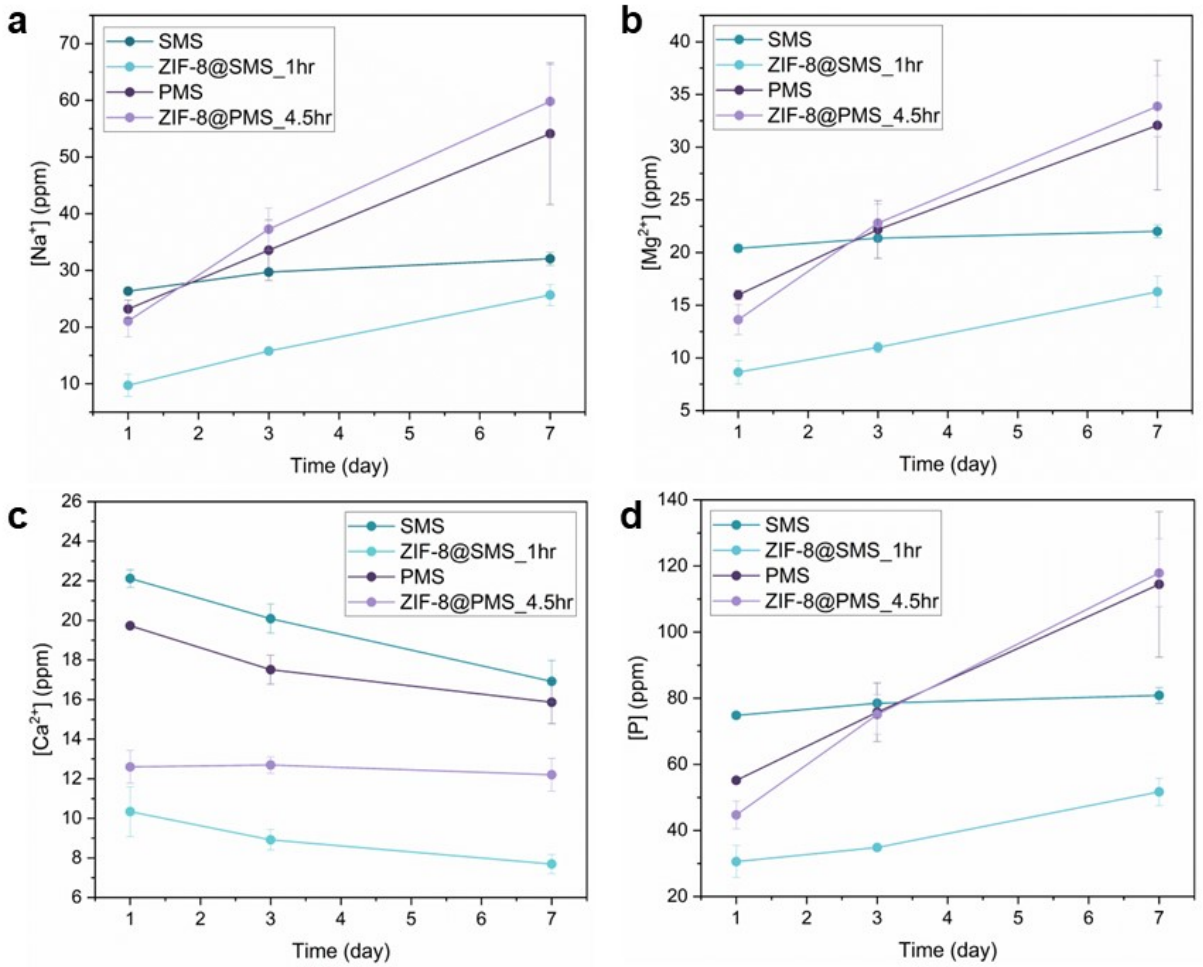

Figure S35. Rate of ion release of the pristine microspheres and composites over a 7-day period, **a.** [Na^+], **b.** [Mg^{2+}], **c.** [Ca^{2+}], and **d.** [P]. [P] refers to all ionic forms of phosphorus (e.g. [PO_4^{3-}], HPO_4^{2-}, $H_2PO_4^-$) detected by ICP-MS.

References

1. N. Ishizawa, H. Setoguchi and K. Yanagisawa, *Sci Rep*, 2013, **3**, 2832.
2. W. Morris, C. J. Stevens, R. E. Taylor, C. Dybowski, O. M. Yaghi and M. A. Garcia-Garibay, *J. Phys. Chem. C*, 2012, **116**, 13307–13312.
3. M. Mozafari, S. Banijamali, F. Baino, S. Kargozar and R. G. Hill, *Acta Biomaterialia*, 2019, **91**, 35–47.